Applied Physics B (2018) 124:76
https://doi.org/10.1007/s00340-018-6947-4

Applied Physics B
Lasers and Optics

LIBS coupled with ICP/OES for the spectral analysis of betel leaves

I. Rehan[1] · K. Rehan[1,2,3] · S. Sultana[4] · M. Z. Khan[1] · R. Muhammad[1]

Received: 29 November 2017 / Accepted: 6 April 2018 / Published online: 13 April 2018

Abstract
Laser-induced breakdown spectroscopy (LIBS) system was optimized and was applied for the elemental analysis and exposure of the heavy metals in betel leaves in air. Pulsed Nd:YAG (1064 nm) in conjunction with a suitable detector (LIBS 2000+, Ocean Optics, Inc) having the optical resolution of 0.06 nm was used to record the emission spectra from 200 to 720 nm. Elements like Al, Ba, Ca, Cr, Cu, P, Fe, K, Mg, Mn, Na, P, S, Sr, and Zn were found to be present in the samples. The abundances of observed elements were calculated through normalized calibration curve method, integrated intensity ratio method, and calibration free-LIBS approach. Quantitative analyses were accomplished under the assumption of local thermodynamic equilibrium (LTE) and optically thin plasma. LIBS findings were validated by comparing its results with the results obtained using a typical analytical technique of inductively coupled plasma-optical emission spectroscopy (ICP/OES). Limit of detection (LOD) of the LIBS system was also estimated for heavy metals.

1 Introduction

The scientific name of betel plant is piper betel. This belongs to the clan of Piperaceae, i.e., the black pepper family [1]. This plant is much more popular in Pakistan. This edible leaf is widely used in countries like Bangladesh, Burma, China, India, Indonesia, Malaysia, Nepal, Philippines, South Africa, Sri Lanka, Thailand, and Pakistan [2]. Traditionally, they are used for chewing in their natural raw circumstance along with many other ingredients like sliced areca nut, slaked lime, coriander, aniseed, clove, cardamom, sweetener, coconut scrapings, ashes of diamond, pearl, gold and silver (ayurvedic preparations), jelly, pepper mint, flavoring agent, and fruit pulp [3]. According to the report of WHO (World Health Organization), frequent use of betel chewing may cause oropharyngeal tumors that may lead to cancer [4].

In the first century of the third millennium in which we are living, scientists are using different techniques for analysis of the elemental composition of edibles [5]. These methods are also very helpful for monitoring pollutants in an adjacent atmosphere such as soil, water and air with which vegetables, farming products and trees are in direct contact. Analysis of elemental composition of edible leaves like betel leaves can provide helpful evaluation and help for the controlled, protected and healthy alimentation [6]. Many of the innovative elemental investigation techniques have been introduced in past spans such as graphite furnace atomic absorption spectrometry (GFAAS) [7, 8], inductively coupled plasma mass spectrometry (ICP-MS) [9, 10], inductively coupled plasma atomic emission spectroscopy (ICP-AES) [11], flame atomic absorption spectroscopy [12, 13], flame atomic absorption spectroscopy [12–14], laser-Induced fluorescence spectroscopy (LIFS) [15, 16] and the most emerging technique of these days is laser-induced breakdown spectroscopy (LIBS) [17, 18]. LIBS is highly applicable to food analysis due to its versatile investigational techniques such as its multi-elemental recognition ability, real-time analysis, ease of implementation, least requirement for sample preparation, high spatial resolution and remote sensing probability [19]. Additionally, every kind of material can be analyzed by LIBS technique irrespective of its nature and matrix (chemical

✉ I. Rehan
irehanyousafzai@gmail.com

[1] Department of Applied Physics, Federal Urdu University of Arts, Science and Technology, Islamabad 44000, Pakistan

[2] State Key Laboratory of Magnetic Resonance and Atomic and Molecular Physics, Wuhan Institute of Physics and Mathematics, CAS, Wuhan 430071, People's Republic of China

[3] School of Physics, University of the Chinese Academy of Sciences, Beijing 100049, People's Republic of China

[4] Department of Chemistry, Islamia College University, Peshawar 25120, Pakistan

composition of element) [20]. Similarly, LIBS is also capable for applications in various interplanetary investigations, elemental analysis of synthetic samples, testing of fertilizers for phosphorous, for quantification of carbon in soil [21–24], qualitative valuations of industrial products for recycling and investigation of materials in harmful surroundings [25], classification of quartz samples [26], for determination of heavy metals in textile dyes [27], as well as for quantitative analysis of Shilajit samples [28].

The aim of present experiment was the application of LIBS as a potential tool for quantitative evaluation of heavy and major elements in edibles (betel leaves) through comparative analysis of LIBS-based analytical approaches and validation accuracy with ICP/OES method. Betel leaves are commonly used for chewing together in a wrapped package of tobacco, spices, along with the mineral slaked lime. We collected the most used edible betel leaves samples from different areas available in Pakistan. The fresh betel leaves were acquired, washed and then dried in desiccators. The dried leaves were crushed to fine powder to prepare pellets and were exposed to laser light to collect emission spectra. To estimate the abundance of the detected elements in the betel leaves samples, we used three different spectroscopic techniques based on LIBS: by standard calibration curve method, integrated intensity ratio method, and by calibration free (CF)-LIBS approach. The LIBS results were validated by comparing to the analyses performed by a more standard analytical technique of inductively coupled plasma/optical emission spectroscopy (ICP/OES). The outcomes by ICP/OES were more precise; but this method needs a lot of time and sample preparation, while LIBS is easy and the outcome may be obtained with nominal sample preparation.

2 Methods and materials

Fresh betel leaves (edible) was purchased from different areas of Pakistan, where these are typically grown. We collected the most used samples of edible betel leaves and named them as sample 1 (Sanchi), sample 2 (Saloon), sample 3 (Pakistani). These leaves were thoroughly scrubbed under tap water and then with distilled–deionized water. The leaves were cut into the small sections (100 g; only leaf portion) and put in a drying oven at 80–85 °C for 3 days for complete dryness. The dried samples were ground to fine particles in aluminum (Al) carbide mortar and dried again at 80–85 °C for 2–3 h, cooled and kept in desiccators. From the powdered material, pellets were made with a graduated, stainless steel, hand-press pellet maker. Before using the mortar and palette maker, they were carefully cleaned to avoid any contamination. Appropriately, strong pellets with smooth surfaces were obtained under these situations.

The present detection setup is exposed in Fig. 1. Briefly, it was composed of an energy source (Laser source), a target holder, and a spectrometer (LIBS2000+, Ocean Optics, USA) with a suitable detector. The experimental setup was assembled and aligned using low power diode laser through Plexiglas mount. Earlier to assembling the experimental setup, all the optics were cleaned thoroughly with isopropyl-alcohol (IPA). A Nd:YAG pulsed laser (1064 nm) was employed as an excitation light supply with a pulse width of 5 ns. The laser pulsed energy was varied utilizing an incorporated capability in the Nd:YAG laser and was calculated via a calibrated energy meter (NOVA-QTL, P/N 1Z01507, Sr. No. 56,461). The laser energy was optimized to be 120 mJ/pulse and was used throughout the experiment. For focusing the laser beam on the surface of target, a convex lens of focal length 200 mm was used. The

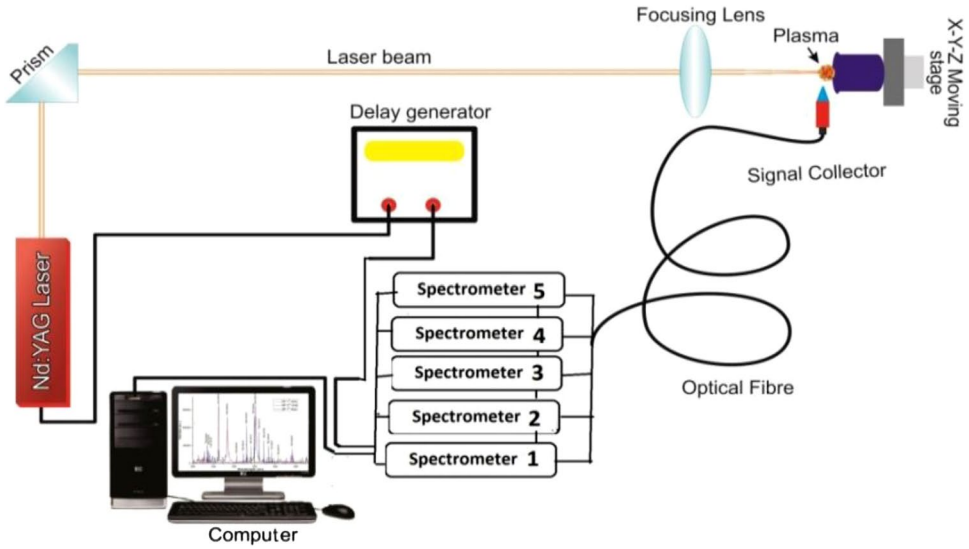

Fig. 1 The experimental layout used in the present study

target was placed at a distance less than the focal length of the focusing lens to prevent any breakdown of ambient air in front of the sample. The emissions from target surface were observed at an angle of 90° to the laser pulse. The LIBS detection system used five spectrometers to measure the amount of light during de-excitation of plasma. The data acquirement time has to be delayed after the excitation which was done through triggering the delay generator via the Q-switched output pulse of the laser as well as via setting a suitable delay for opening of the acquirement time for the set interval. In our case, the optimum time delay was observed between 200 and 600 ns. The plasma emissions resulting from sample ablation were collected using fiber probe attached to an optical fiber transmit it via a 10 µm slit to a high resolution spectrometer (LIBS2000+, Ocean Optics, USA). The LIBS2000 + detection system was outfitted with five HR2000 small spectrometers each having different numbers of grooves on the grating (1800 lines/mm and 2400 lines/mm to cover the spectral region from 200 to 700 nm). All of the spectrometers have 2048 element linear CCD arrays having an optical resolution of about 0.06 nm with the capacity to work at different delay times. The integration time of detector was kept at 2.1 ms.

The spot size on the sample due to laser beam was measured from the burn pattern on the polaroid sheet to about ~ 300 µm, from which the laser fluency was estimated to be ~ 169 J/cm^2. To regulate the delay time, the CCD camera was synchronized and was set to 300 ns in the current experiment. All the emissions spectra were acquired utilizing a single laser shot and then taking an average of 30 such spectra to obtain the best S-to-N ratio. The spectrometer was turned on and first of all, a dark spectrum was recorded (mainly coming from the instrumental and background noise) and then it was subtracted from all the spectra recorded under specific experimental conditions before saving. The lowest detection limit of LIBS was determined using [29–31]

$$\mathrm{LOD} = \frac{2\sigma}{S} \tag{1}$$

where σ stands for the standard departure of the calibrated data, and S stands for the slope of the calibration curve. To calibrate the wavelength scale, a low-pressure Hg-lamp (Ocean optics) was used. From scanning a narrow line width dye laser, the instrumental bandwidth has been calculated to be on the average ~ 0.05 ± 0.01 nm. The manipulations of LIBS spectra were performed through Origin Pro-08 software program that permits the qualitative as well as quantitative measurements of the elemental constitution of target samples.

For LIBS analysis, the collected samples were first converted into pellets by putting 10 gm of sample in a dye and pressing them by applying a load of 10 tons for 20 min in the dimensions ~ 4 cm × 6 cm and a thickness of ~ 2 cm and were pasted on target stand for ablation.

To study the betel leaves for heavy and major elements via ICP/OES, standard operating procedure (SOP) for digestion and analysis based on Environmental and Protection Agency (EPA) was performed. Digestion process of test samples in different acids was carried out to transform samples into solutions, and for this purpose, about 0.5 g of fine dried powder sample was weighted using an analytical balance and dissolved in concentrated HNO_3 that was lifted for 24 h for proper dissolution of metals in acid. 10 mL of $HClO_4$ was added and the mixture was heated between (280–300) °C. During heating, 2–3 mL of H_2O_2 was added in slowly to obtain a clear solution. The solution was then filtered and analyzed via ICP- spectrometer (OPTIMA 2100-DV; PerkinElmer, Twofold View).

3 Results and discussion

3.1 Emission studies

The plasmas of betel leaves were generated by the first harmonic laser output @ 1064 nm of Nd: YAG laser at ambient air environment. The emission spectra were recorded using a multichannel spectrometer in the spectral range 200–720 nm. The detector was positioned at ≈ 0.5 mm from the sample surface, at an angle of 90° to the expansion of plasma plume direction. The detector position was tested for different angles and when the detector was placed at 90° to the plume direction, then signals with maximum intensities were obtained. Therefore, the angle 90° was used throughout the experiments. In general, multi-pulse analysis via averaging of the emission spectra was employed in LIBS examination for the purpose of reducing the unwanted experimental fluctuations and to improve the S-to-N ratio, that usually comes from laser power variation. In the present experiment, the spectral emissions were averaged for 30 laser shots. A typical emission spectrum of sample 1 is exposed in Fig. 2.

The spectrum shows well-isolated spectral emission lines with small background field. The spectral emissions lines were recognized via the National Institute of Standards and Technology (NIST) database [32]. The attentive analysis exposed the existence of many neutral/ excited spectral emissions and spectral emission lines conforming different ionized states corresponding to different elements like aluminum, barium, calcium, copper, magnesium, manganese, sodium, phosphorous, strontium, sulfur, potassium, iron and zinc. To produce laser ablations at the surface of target samples, the samples were placed in a vacuum chamber. Although the spectra were obtained at atmospheric pressure, but due to limited availability of atmospheric hydrogen inside chamber, we were unable to have H_α line in the

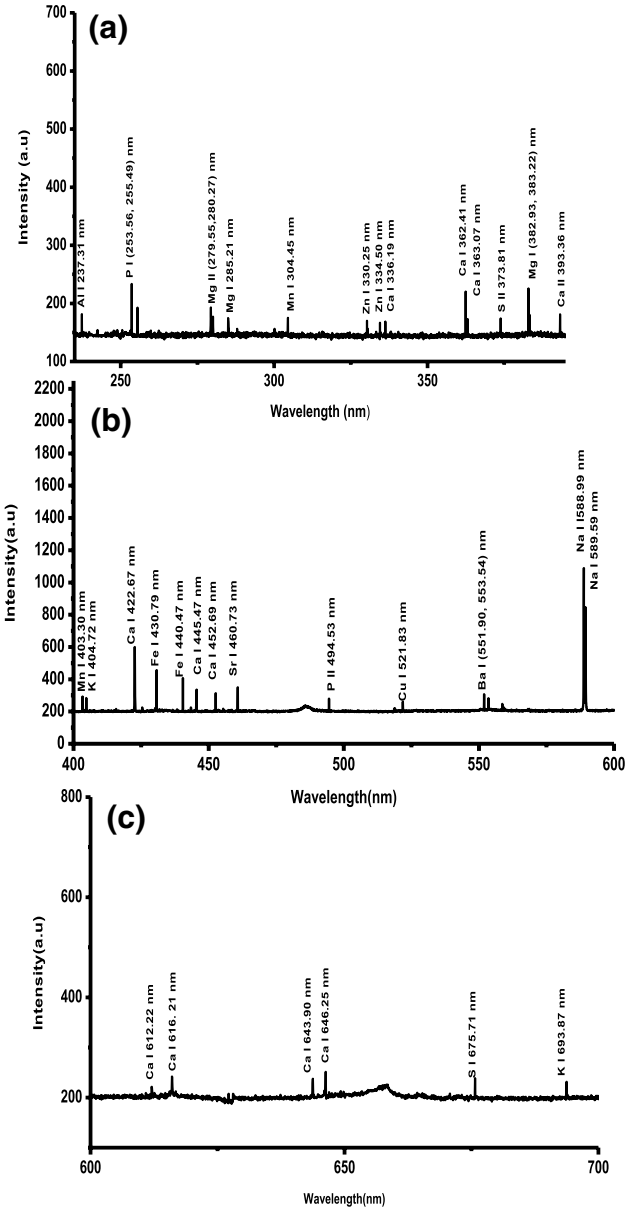

Fig. 2 **a**–**c** The typical LIBS spectrum of sample 1

emission spectra. Confirmations of our results were done via comparison of LIBS spectra of target sample with the spectral emissions of the pure elements employing the same methodology.

3.2 Parameters of laser-induced plasma (electron temperature and electron density)

To study the plasma properties and to perform both quantitative and qualitative analysis, the study of spectral emissions from laser-produced plasma is very significant. The fundamental properties of plasma are electron temperature (T_e) and electron number density (N_e). The measurement of plasma parameters is tremendously important to validate the assumption of optically thin plasma (OTP) and the local thermodynamic equilibrium (LTE) which are crucial for the LIBS quantitative analysis. In case, the plasma does not verify the LTE condition, it shows the presence of strong self-absorption and as a consequence, the quantitative analysis of target will be incorrect. Furthermore, the understanding of electron temperature is important to know the process occurring during production of plasma such as atomization, dissociation, and excitation. It also helps to improve the sensitivity of LIBS. One of the main significant conditions that satisfy that plasma is in the state of LTE is that the collisional process occurring in the plasma dominates the radiative process. The most frequent criteria used to approximate LTE supposition is the McWhirter criterion. This criteria justifies when the rate of collisional process dominates over the radiative process as,

$$N_e \geq 1.6 \times 10^{12} T_e^{1/2} (\Delta E)^3 \tag{2}$$

where T_e (K) is the electron temperature, ΔE (eV) gives the energy difference of oscillations responsible for spectral emission associated, and N_e (cm^{-3}) shows the electron density.

The electron temperature can be approximated using the Boltzmann eqn.

$$ln\left(\frac{I\lambda}{Ag}\right) = -\frac{E_i}{kT_e} + ln\left(\frac{4\pi U(T)}{hcN_l}\right) \tag{3}$$

where I stand for the LIBS signal intensity, A (s^{-1}) is transition probability, E_i is the energy of upper level. U gives the partition function, h is plank's constant, c gives the speed of light, and N_l is the population density of ground state. The parameters A, g, E_i, and $U(T)$ were obtained from NIST atomic database and Kurucz atomic spectral lines database [33]. By plotting the left side of Eq. (3) against E_i,, the electron temperature can be estimated from the slope of the straight line (-1/KT). Different important conditions must be satisfied such as (1) the separation between wavelengths should be very small to avoid the corrections due to relative response of the detector (2) the energy separation in upper excited levels should be as large as possible to increase the precision and (3) the lines must not be optically thick. A typical Boltzmann plot (sample 1) using Ca-I emission lines is exposed in Fig. 4. The Boltzmann plot plotted using Ca-I spectral lines at 336.19, 445.47, 452.69, 612.22, and 616.21 nm. Calcium lines were used to measure the plasma temperature, as the selected spectral lines having more than two different energy levels needs to be clearly observed and Ca I lines fulfill this condition with the setup used in the present work. The LTE condition was justified by estimating the electron density (N_e) through the Stark-broadened lines

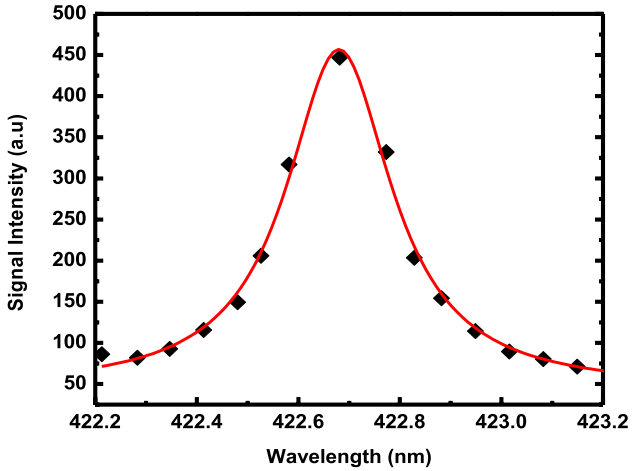

Fig. 3 Lorentzian fitted line profile of Ca I at 422.67 nm corresponding to ($3p^6\ 4s^2\ ^1S_0 \rightarrow 3p^6 4s4p\ ^1P^0_1$) transition using sample 1

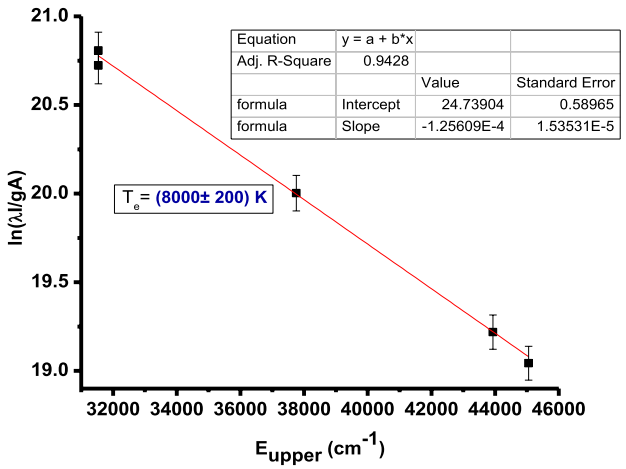

Fig. 4 Typical Boltzmann plot using neutral Ca emission lines from sample 1. The continuous line shows best linear fit

profile for Ca-I spectral line at wavelength 422.67 nm as depicted in Fig. 3. The N_e was determined using the relation,

$$N_e(\mathrm{cm}^{-3}) = \left(\frac{\Delta\lambda_{\frac{1}{2}}}{2\omega}\right) \times 10^{16} \tag{4}$$

where ω gives the "electron impact parameter" [34]. The correct value of $\Delta\lambda_{1/2}$ was achieved by subtracting the effect of instrumental broadening, via the relation,

$$\Delta\lambda_{\mathrm{correct}} = \Delta\lambda_{\mathrm{obser}} - \Delta\lambda_{\mathrm{instr}} \tag{5}$$

The measured value of N_e was ~ 1.5×10^{18} cm^{-3}.

The plasma temperature estimated by the Boltzmann plot method was (8000 ± 200) K. This value of electron temperature used in the mathematical formula for McWhirter's criterion along with value of difference of energy between the associated energy levels of respected transition of calcium neutral emission line at wavelength 422.67 nm furnishes the electron number density of about 3.6×10^{15} cm^{-3} that was less than the value determined experimentally and hence shows the agreement of the McWhirter's criterion. This implies that plasma was near to LTE. In the same way, T_e and N_e determined for all spectra were found to be similar under ± 10% uncertainty. The McWhirter's criteria was tested and verified for spectra of all the samples. For further information, the plasma temperature was also estimated using Mg I spectral lines at [285.2, 382.9, and 383.2] nm and found to be 7207 ± 200 K, thereby yielding an average plasma temperature of ~ 7584 ± 200 K.

4 LIBS optimization

While using LIBS, the time delay between the laser excitation and data acquirement is relatively critical, because it plays a major role in the generation of an explicit atomic transition lines with least broadening and overlapping. After excitation at the early on stage, the electrons and ions are colliding with one another, resulting the broadening and overlapping of atomic and ionic emissions lines [35]. For the intention to reduce this effect and to get considerable spectral transition lines, the time span between the generation and the signal attainment was optimized, so that the peaks of spectral emissions were well-resolved without compromising on S-to-N ratio. The laser pulse energy is an essential parameter to be optimized in the LIBS method. The intensity of LIBS signal increases linearly versus laser pulse energy until the earlier gets saturated at a critical value of laser pulse energy (see Fig. 5). The early linear dependency was due to the increase of ablated material from the material's surface due to high pulse energy. The increase of laser energy, also results in the increase of plasma temperature, and above a critical value of laser energy, the free electrons in the hot plasma absorb laser photons and this effect is called inverse Bremsstralung effect (IB) [36]. When laser interacts with the sample, the ablation is done by leading portion of the laser pulse, and is not dependent of laser energy, whereas the preceding plasma heating is carried out by the remaining part of the laser pulse either during the process of IB or during photo ionization (PI) rather than pairing with the target. The IB effect is strongly wavelength dependent that increases with the wavelength and thus, in our case, as excitation of the emission.

The effects of lens distance on focusing signal intensity was also optimized while performing our experiments as exposed in Fig. 6.

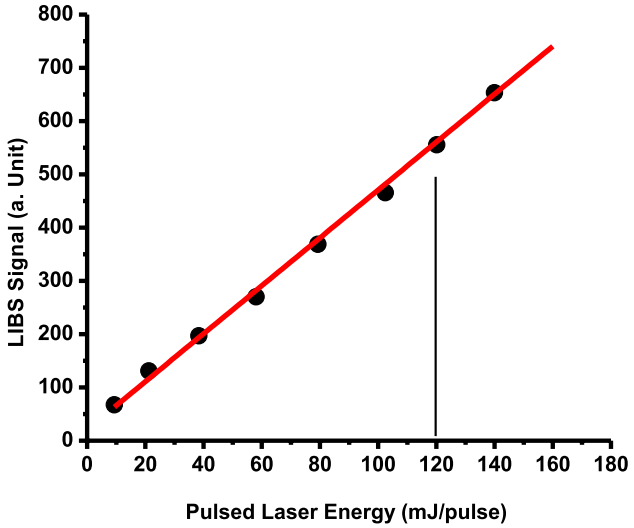

Fig. 5 LIBS signal intensity against laser pulse energy for Fe-I 430.79 nm atomic emission line

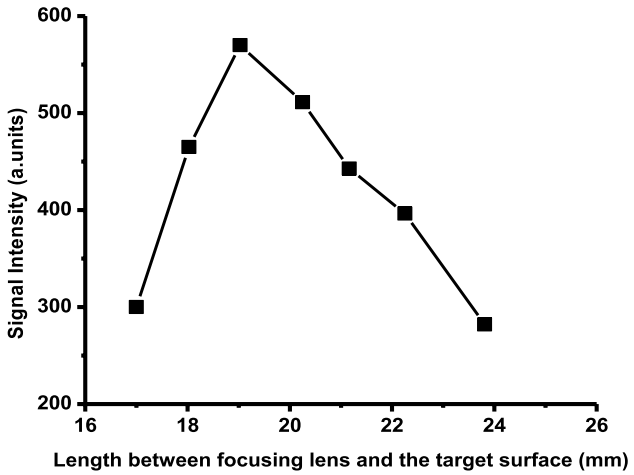

Fig. 6 The effect of lens distance on the intensity of incident signal using Fe-I at 430.79 nm

5 Quantitative analysis

5.1 Calibration curves method

For estimation of the concentration of detected elements present in betel leaves samples, three calibration approaches based on LIBS were used, i.e., the standard calibration curve method, integrated intensity ratio method, and CF-LIBS approach. The quantitative measurements of heavy and trace metals present in the betel leaves were carried out by selecting the atomic lines, Al-I 237.31 nm, Ca-I 643.90 nm, Cu-I 521.83 nm, Cr-I 425.43 nm, Sr-I 460.73 nm, Mg-I 285.21 nm, Mn-I 403.30 nm, P-I 253.56 nm, Fe-I 440.47 nm, Zn-I 330.25 nm, Ba-I 553.54 nm, Na-I 588.99 nm, K I at 404.72 nm, and S-II 373.81 nm. Those particular atomic transition lines were chosen for the reason that they were strongly intense, isolated and well-resolved atomic transition lines in the spectral region.

In LIBS quantitative investigation, the quantification of different elements in a given sample can be carried out via the intensities of spectral emission line (ionic as well as atomic). Calibration curves can be constructed based on some set of samples (normally more than three) with different standard concentrations of a particular analyte. These curves give a way to approximate the abundance of particular elements in an unknown target. The graph of spectral peak intensities of a specific element against its concentration provides a calibration curve. For calibration purposes, all the detected elements were used. All these elements were obtained in powder form with about 99.99% purity. Metals in powder form were mixed in the betel leaves matrix in a ball milling apparatus to good mixing and homogeneity. To check the homogeneity of our samples, several LIBS measurements were performed at different locations at the surfaces of the pallets. Different standard samples of known concentrations like 50, 100, 200, 400, 800 and 1600 ppm, of elements under study were prepared and LIBS spectra were recorded for these six concentrations of every element under optimized parameters. We choose normalized LIBS intensity. Figure 7 exposed the calibration curves for quantification of Al, and P from sample 1.

The calibration curves were normalized with respect to potassium due to the reason of most abundance of K in all of the analyzed samples. The estimated concentration of detected elements in betel leaves using calibration curves method was tabulated in Table 1 and plotted as in Fig. 8a–c.

5.2 Integrated intensity ratio method

Integrated intensity of an element is a given sample is proportional to the concentration of a specified element in a given sample. In this methodology, the concentration of an unknown element was calculated with respect to the sum of all intensities of all the elements present in the sample. The relative concentrations of elements in betel leaves via the integrated intensity ratio method were tabulated in Table 1 and plotted in Fig. 8a–c.

5.3 Calibration free-LIBS method

The third technique was calibration free-LIBS approach. Several experimental conditions should be fulfilled prior to applying this technique [37].

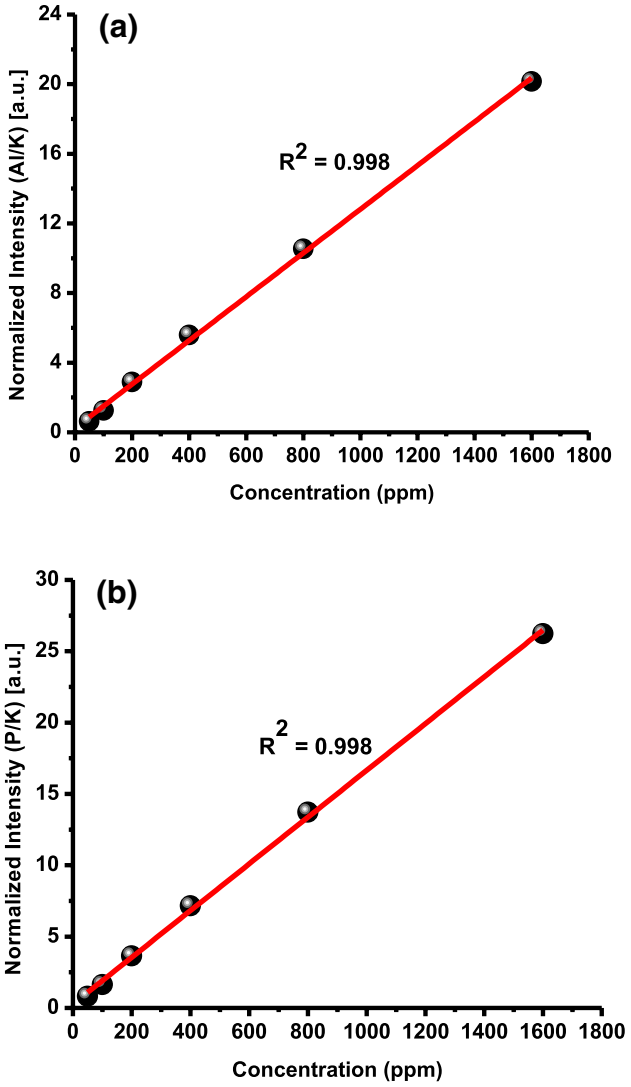

Fig. 7 **a**–**b** Typical calibration curves for Al, and P from sample 1 using normalized intensity with K. The highest value of R-squared factor shows the best linear fitting

- The laser power density must be large so as to produce stoichiometric ablation.
- Laser plasma must not be optically thick to evade/reduce self-absorption in the emission lines.
- The condition of local thermal equilibrium (LTE) must be satisfied.

5.3.1 (CF)-LIBS algorithm

The process of (CF)-LIBS calculations are as follows;

- Analyze the LIBS spectra.
- Calculate the T_e by Boltzmann plot for each element (using Eq. 3).
- Calculate the partition function.
- Calculate the experimental factor F through the normalization of the sum of the elemental concentrations as $\sum C = 1$.
- Then, use the relation $q = \ln\left(\frac{\mathrm{FC}}{U(T)}\right)$ to determine the abundance "C" of each element.

The detailed explanation of (CF)-LIBS methodology was already given in detail in our previous work [38].

5.3.2 Stoichiometric-ablation and optically thin plasma

The determination of laser power density at the focal spot on the surface of target was necessary to verify the stoichiometric ablation. The power density at the corresponding laser energy of 120 mJ was of the order of 10^{11} W/cm^2, which was sufficient to produce stoichiometric ablation at the surface of sample [39]. For optically thin plasma, the ratio of intensities of two isolated spectral lines of an element measured experimentally should be nearly the same as the ratio of the theoretically measured intensities as,

$$\frac{I}{I'} = \frac{A_1 g_1 \lambda_2}{A_2 g_2 \lambda_1} \exp\left(\frac{-(\Delta E)}{kT_e}\right) \tag{6}$$

To check this condition, we determined intensity ratios spectral lines from Ca and Mg. The ratio of Ca-I (362.41 nm) and Ca-I (363.07) nm was 1.32, whereas the ratio of their related transition probabilities was 1.38. In the same way, the ratio of Mg I (382.9) nm and Mg-I (383.2) nm was 1.32 and that of related transition probabilities was 1.39. This consistency supported our assumption of optically thin plasma.

The relative concentrations of elements in betel leaves via CF-LIBS method were tabulated in Table 1 and plotted in Fig. 8a–c. We confirmed our findings by comparing the concentrations of analyzed elements with more standard analytical technique namely ICP/OES. Elements detected in betel leaves and comparison of concentration detected with LIBS and ICP were exposed in Table 1 [40].

In the present work, ICP/OES was used as a standard analytical tool. The results of LIBS and ICP/OES were compared which shows that LIBS (Normalized Calibration curves) method gives close output to that of ICP Spectroscopy.

The studied samples were found to be composed of more than 13 different elements in which 5 are heavy metals (Ba, Cr, Cu, Mn, and Zn). Some of the elements like Al, Ba, Cu, Cr, S, and Zn were higher than the permissible safe limits. For example, in the sample under analysis, the concentration of Al = 89–480 ppm, Ba = 29–98.25 ppm, Cu = 10–12.5 ppm, Cr = 2.5–3.5 ppm, S = 1367–1791.10 ppm, and Zn = 16–23.69 ppm, while the maximum permissible limits set by WHO for these elements are: Al = 30 ppm, Ba = 2 ppm,

Table 1 The comparison of LIBS with ICP for different elements detected in betel leaves

Elements	Wavelength (nm)	LIBS (ppm)			ICP/OES (ppm)
		Calibration curve method	Calibration free-LIBS method	Integrated intensity ratio method	
Sample 1					
Al	237.31	132.30 ± 2.64	137.25 ± 2.74	139.13 ± 2.78	126.50 ± 2.53
Ba	553.54	98.25 ± 4.91	103.31 ± 5.16	102.39 ± 5.11	90.79 ± 4.53
Ca	643.90	31987 ± 639.74	33256 ± 665.12	33990 ± 679.80	29991 ± 599.82
Cu	521.83	12.69 ± 0.63	13.78 ± 0.68	13.99 ± 0.69	11.64 ± 0.58
Fe	440.47	147.95 ± 2.95	149.99 ± 2.99	151.26 ± 3.02	142.93 ± 2.85
K	404.72	68750.29 ± 1375	69980.79 ± 1399.60	70021.81 ± 1400.43	65784.86 ± 1315.69
Mg	285.21	14950.20 ± 299	15859.15 ± 317.18	16123.12 ± 322.46	13896.20 ± 277.92
Mn	403.30	175.15 ± 3.50	179.27 ± 3.58	178.14 ± 3.56	170.09 ± 3.40
Na	588.99	800.91 ± 16.01	802.52 ± 16.05	803.98 ± 16.07	791.88 ± 15.83
P	253.56	12893.40 ± 257.86	13791.51 ± 275.83	14051.29 ± 281.02	11910.36 ± 238.20
S	373.81	1791.10 ± 35.82	1801.21 ± 36.02	1825.25 ± 36.50	1700.39 ± 34
Sr	460.73	73.81 ± 3.69	74.98 ± 3.74	75.10 ± 3.75	71.84 ± 3.59
Zn	330.25	23.69 ± 1.18	27.58 ± 1.37	26.89 ± 1.34	21.59 ± 1.07
Sample 2					
Al	237.31	89 ± 4.45	91 ± 4.55	90 ± 4.50	87 ± 4.35
Ba	553.54	29 ± 1.45	30 ± 1.50	31 ± 1.55	28 ± 1.4
Ca	643.90	31470 ± 629.40	31780 ± 635.60	31,900 ± 638	31314 ± 626.28
Cr	425.43	2.5 ± 0.12	2.8 ± 0.14	3.0 ± 0.15	2 ± 0.10
Cu	521.83	12.5 ± 0.62	13 ± 0.65	13.7 ± 0.68	12 ± 0.60
Fe	440.47	80 ± 4.00	82 ± 4.10	83.5 ± 4.17	78 ± 3.90
K	404.72	43801 ± 876.02	44,000 ± 880	44,500 ± 890	43612 ± 872.24
Mg	285.21	17009 ± 340.18	17501 ± 350.02	17890 ± 357.80	16921 ± 338.42
Mn	403.30	38 ± 1.90	40 ± 2.00	40.5 ± 2.02	36 ± 1.80
Na	588.99	3083 ± 61.66	3090 ± 61.80	3100 ± 62	3053 ± 61.06
P	253.56	1991 ± 39.82	2050 ± 41	2099 ± 41.98	1988 ± 39.76
S	373.81	1367 ± 27.34	1381 ± 27.62	1395 ± 27.90	1347 ± 26.94
Sr	460.73	127 ± 2.54	129 ± 2.58	128.8 ± 2.57	124 ± 2.48
Zn	330.25	16 ± 0.80	17 ± 0.85	17.5 ± 0.87	15 ± 0.75
Sample 3					
Al	237.31	480 ± 9.60	485 ± 9.70	489 ± 9.78	475 ± 9.50
Ba	253.54	68 ± 3.40	70 ± 3.50	71 ± 3.50	67 ± 3.35
Ca	643.90	31699 ± 633.98	31,900 ± 638	32,500 ± 650	31,500 ± 630
Cr	425.43	3.5 ± 0.17	4 ± 0.20	4.4 ± 0.22	3 ± 0.15
Cu	521.83	10 ± 0.50	10.7 ± 0.53	11 ± 0.55	9 ± 0.45
Fe	440.47	415 ± 8.30	429 ± 8.58	431 ± 8.62	404 ± 8.08
K	404.72	79885 ± 1597.70	80,000 ± 1600	83099 ± 1661.98	79819 ± 1596.38
Mg	285.21	5675 ± 113.50	5800 ± 116	6000 ± 120	5500 ± 110
Mn	403.30	24 ± 1.20	26 ± 1.30	27 ± 1.35	22 ± 1.10
Na	588.99	2367 ± 47.34	2389 ± 47.78	2395 ± 47.90	2347 ± 46.94
P	253.56	2969 ± 59.38	2978 ± 59.56	3250 ± 65	2850 ± 57
S	373.81	1405 ± 28.1	1450 ± 29	1550 ± 31	1394 ± 27.88
Sr	460.73	125 ± 2.50	137 ± 2.74	148 ± 2.96	117 ± 2.34
Zn	330.25	17 ± 0.85	18 ± 0.90	18.5 ± 0.92	16 ± 0.80

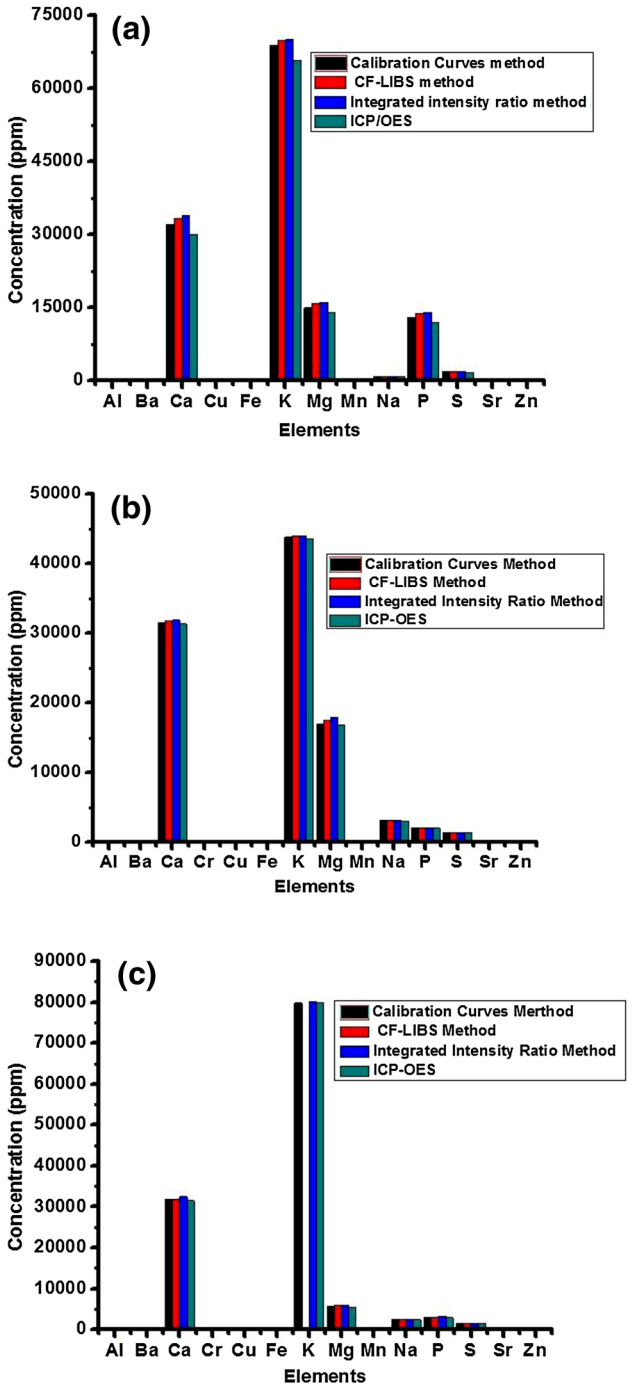

Fig. 8 **a**–**c** Comparison of concentration of detected elements in sample 1, 2, 3 using three LIBS-based approaches and ICP/OES

Cu = 0.00083, Cr = 1 ppm, S = 800 ppm, and Zn = 18 ppm, respectively. Chromium was not detected in sample 1. Zn was above the permissible safe limit in sample 1 only. The analyzed samples were found to be rich in potassium. Other heavy metals like Ni, Ti, Hg, and Pb were below the detectable limits of present experimental setup. The present study shows that the elemental composition of betel leaves collected from various locations varies from sample to sample. The LOD for Cr, Cu, and Zn were found to be 1, 4, and 6 ppm, respectively.

6 Conclusions

Spectral analyses of betel leaves were performed by LIBS to measure the concentrations of heavy and essential metals in the samples. Elements like Al, Ba, Ca, Cr, Cu, Fe, K, Mg, Mn, Na, P, S, Sr, and Zn were confirmed to be present in betel leaves. The comparative study of LIBS with ICP/OES showed that using the normalized calibration curves method yielded the closest outcomes to the values provided by ICP/OES. To increase the sensitivity of LIBS system and to get best limit of detection, the detection system was optimized in terms of laser energy and focusing lens distance from target surface. Quantitative determinations were carried out under the LTE and optically thin plasma assumptions. The heavy metals like Ba, Cr, Cu, and Zn were found to be above the permissible safe limits in all the samples. The results of LIBS were cross-validated by comparing the results with the results of a more standard analytical technique of ICP/OES and were found to be in good harmony. The results by ICP/OES were more precise, but this method requires more time and laborious sample preparation, whereas LIBS is easy and the results can be acquired with minimum sample preparation. Furthermore, limit of detection (LOD) of LIBS setup was also determined for Cr, Cu, and Zn.

References

1. J. Gunther, Eisenhower: the man and the symbol (Harper, 1952)
2. S. Sadhukhan, P. Guha, AMA-Agricultural Mechanization in Asia Africa and Latin America **42**, 47 (2011)
3. W.S. Eipeson, J. Manjunatha, P. Srinivas, T.S. Kanya, Ind. Crops Prod. **32**, 118 (2010)
4. WHO E. C. o. t. P. o. Cancer, Prevention of Cancer: Report (World Health Organization, 1964)
5. S. Delibacak, O. Elmaci, M. Secer, A. Bodur, Int. J. Water **2**, 196 (2002)
6. J.-C. Leblanc, T. Guérin, L. Noël, G. Calamassi-Tran, J.-L. Volatier, P. Verger, Food Additives Contam. **22**, 624 (2005)
7. ÉC. Lima, F. Barbosa Jr., F.J. Krug, Fresenius' J. Anal. Chem. **369**, 496 (2001)
8. D. Santos, F. Barbosa, A. Tomazelli, F. Krug, J. N˙brega, M. Arruda, Anal. Bioanal. Chem. **373**, 183 (2002)
9. K.C. Chan, Y.C. Yip, H.S. Chu, W.C. Sham, J. AOAC Int. **89**, 469 (2006)
10. Y. Şahan, F. Basoglu, S. Gücer, Food Chem. **105**, 395 (2007)
11. C.S. Kira, V.A. Maihara, Food Chem. **100**, 390 (2007)
12. G. Doner, A. Ege, Analytica Chimica Acta **520**, 217 (2004)
13. S. Saracoglu, K.O. Saygi, O.D. Uluozlu, M. Tuzen, M. Soylak, Food Chem. **105**, 280 (2007)
14. M. Tuzen, M. Soylak, Food Chem. **102**, 1089 (2007)
15. R. Karoui, C. Blecker, Food Bioprocess Technol. **4**, 364 (2011)
16. H.K. Noh, R. Lu, Postharvest Biol. Technol. **43**, 193 (2007)

17. D.A. Cremers, F.Y. Yueh, J.P. Singh, H. Zhang, Encyclopedia of analytical chemistry (2006)
18. A.W. Miziolek, V. Palleschi, I. Schechter, Laser induced breakdown spectroscopy (Cambridge University Press, 2006)
19. I. Rehan, K. Rehan, S. Sultana, M.O. ul Haq, M.Z.K. Niazi, R. Muhammad, Eur. Phys. J. Appl. Phys. **73**, 10701 (2016)
20. G. Senesi, M. Dell'Aglio, R. Gaudiuso, A. De Giacomo, C. Zaccone, O. De Pascale, T. Miano, M. Capitelli, Environ. Res. **109**, 413 (2009)
21. F. Colao, R. Fantoni, V. Lazic, A. Paolini, F. Fabbri, G. Ori, L. Marinangeli, A. Baliva, Planet. Space Sci. **52**, 117 (2004)
22. G. Nicolodelli, G. Senesi, R. Romano, J. Cabral, I. Perazzoli, B. Marangoni, P. Villas-Boas, D. Milori, Appl. Phys. B **123**, 127 (2017)
23. B.S. Marangoni, K.S.G. Silva, G. Nicolodelli, G.S. Senesi, J.S. Cabral, P.R. Villas-Boas, C.S. Silva, P.C. Teixeira, A.R.A. Nogueira, V.M. Benitesf, and D. M. B. P. Milorib, Anal. Methods **8**, 78 (2016)
24. G. Nicolodelli, B.S. Marangoni, J.S. Cabral, P.R. Villas-Boas, G.S. Senesi, C.H.D. Santos, R.A. Romano, A. Segnini, Y. Lucas, C.R. Montes, and D. M. B. P. Milori, Applied optics **53**, 2170 (2014)
25. B. Carranza, G. Fisher, D. Yoder, Hahn, Spectrochimica Acta Part B: Atomic Spectroscopy **56**, 851 (2001)
26. A. Ali, M.Z. Khan, I. Rehan, K. Rehan, R. Muhammad, J. Spectrosc. **2016** (2016)
27. I. Rehan, Rehan, and S. Sultana
28. I. Rehan, R. Muhammad, K. Rehan, K. Karim, and S. Sultana, J. Nutr. Food Sci. **07** (2017)
29. I. Rehan, M.Z. Khan, I. Ali, K. Rehan, S. Sultana, S. Shah, Appl. Phys. B **124**, 49 (2018)
30. M.A.Gondal, T. Hussain, Z.H. Yamani, M.A. Baig, Talanta **69**, 1072 (2006)
31. M.A. Gondal, T. Hussain, Z.H. Yamani, Z. Ahmed, Bull. Environ. Contamination Toxicol. **78**, 270 (2007)
32. Y. Ralchenko, F.C. Jou, D.E. Kelleher, A. Kramida, A. Musgrove, J. Reader, W.L. Wiese, K. J. Olsen http://physics.nist.gov/asd3 (2005)
33. W. Martin, J. Fuhr, D. Kelleher, (National Institute of Standards and Technology, Gaithersburg, MD, 2002)
34. H.R. Griem, Principles of plasma spectroscopy (Cambridge University Press, 2005)
35. D. Heading, J. Wark, G. Bennett, R. Lee, J. Quant. Spectrosc. Radiative Transfer **54**, 167 (1995)
36. A.A.I. Khalil, M.A. Gondal, M. Shemis, I.S. Khan, Appl. Optics **54**, 2123 (2015)
37. A. Ciucci, M. Corsi, V. Palleschi, S. Rastelli, A. Salvetti, E. Tognoni, Appl. Spectrosc. **53**, 960 (1999)
38. I. Rehan, K. Rehan, S. Sultana, M.Z. Khan, Z. Farooq, A. Mateen, M. Humayun, Int. J. Spectrosc. **9** (2017)
39. E. Tognoni, G. Cristoforetti, S. Legnaioli, V. Palleschi, Spectrochimica Acta Part B: Atomic Spectroscopy **65**, 1 (2010)
40. I. Rehan, M.A. Gondal, K. Rehan, Determination of lead content in drilling fueled soil using laser induced spectral analysis and its cross validation using ICP/OES method. Talanta **182**, 443–449 (2018)